

Parallel MRI Reconstruction Using Broad Learning System

Yuchou Chang and Ukash Nakarmi, *Member, IEEE*

Abstract— As an inverse problem, parallel magnetic resonance imaging (pMRI) reconstruction accelerates imaging speed by interpolating missing k-space data from a group of phased-array coils. Deep learning methods have been used for improving pMRI reconstruction quality in recent years. However, deep learning approaches need a large amount of training data that are acquired from different hardware configurations and anatomical areas. Data distributions may be different between training data and testing data, and a long-time training is needed. In this work, we proposed a broad learning system based parallel MRI reconstruction that exploits approximation capability of one-layer neural network through broadening network structure with expanded nodes. Experimental results show that the proposed method is able to suppress noise in compared to the conventional pMRI reconstruction.

I. INTRODUCTION

Magnetic resonance imaging (MRI) is inherently slower compared to other medical imaging modalities. Long data acquisition time in MRI pertains to its sequential data acquisition protocol and physical constraints. Slow imaging speed causes not only compromise and limits image resolution and capabilities but also increased costs and causes patient discomfort [1]. For these reasons, accelerating MR data acquisition process has been of perennial interest. Parallel MRI (pMRI) technique [2] accelerates MRI imaging speed by partial data acquisition through k-space undersampling. In pMRI, a group of phased-array coils are used to acquire a reduced amount of k-space data and missing data are reconstructed using acquired data from multiple coils. Due to undersampled data acquisition, Nyquist sampling rate criterion is violated and results in aliased images, which necessitates dedicated reconstruction techniques in pMRI.

Parallel MRI reconstruction techniques can be classified as image-based [3], k-space-based [4], and combinations of previous two kinds of methods [5]. In compared to image-based methods, k-space-based methods don't need to estimate sensitivity profiles from an array of coils, so that incorrect estimation of coil sensitivity could be avoided. A typical k-space-based pMRI reconstruction method is GRAPPA [4]. For k-space-based methods, more accurate interpolation strategies for reconstructing missing k-space data produces better reconstruction quality. Henceforth, a number of methods have been proposed to improve interpolation accuracy for estimating missing k-space data, hence, reducing aliasing artifacts and enhancing signal to noise ratio (SNR). Recently, deep learning methods have been used to enhance interpolation accuracy in k-space-based pMRI reconstruction methods. For example, A robust artificial neural network for k-space interpolation (RAKI) [6] was proposed using

convolutional neural network (CNN) training on autocalibrating signal (ACS) data and then the trained model interpolates missing k-space data. DeepSPIRiT also used CNN trained on a large database of normalized k-space data using coil compression [7]. Another convolutional neural network: U-Net was trained on a knee k-space dataset and Human Connectome Project (HCP) MR dataset to interpolate the missing k-space data using low-rank Hankel matrix completion [8]. Neural network has been successfully used to solve the inverse problem in deep MRI reconstruction [9].

MRI data acquisition is costly in compared to natural image acquisition, and therefore have limited training databases [10]. Deep learning models are data-hungry, and their performance drops precipitously with the decrease in the training data size. Transfer learning models are efficient in several domains to address data-scarcity problems in deep-learning based techniques [11]. However, in medical imaging, particularly in MRI, training data and testing data may have different distributions in source and target domains under transfer learning framework [12]. Moreover, MR coil architectures and images from different MR scanner vendors may have different characteristics and features making transfer learning inefficient. Broad learning system (BLS) was developed recently for classification and regression tasks using one-layer neural network [13]. BLS in one hand reduces the size of training data set required while on the other eliminates the complexity and long training process prevalent in deep neural networks, consequence of BLS's simple architecture. In this paper, a broad learning system (BLS) is investigated for improving interpolation accuracy in GRAPPA reconstruction. The proposed method doesn't require extra training data to build an offline training model. The paper is organized as following. Motivation and background introduction are presented in the sections I and II. The section III provides the proposed method. Experimental results and conclusion are given in the sections IV and V.

II. RELATED BACKGROUND

A. GRAPPA Reconstruction

GRAPPA reconstruction [4] is generalized as an interpolation process to estimate missing k-space data as the following equation (1):

$$S_j(k_y + r \cdot \Delta k_y, k_x) = \sum_{l=1}^L \sum_{b=-N_b}^{N_a} \sum_{h=-H_l}^{H_r} w_{j,r}(l, b, h) \times S_l(k_y + b \cdot R \cdot \Delta k_y, k_x + h \cdot \Delta k_x) \quad (1)$$

, where S represents k-space signals, w denotes the weight coefficients estimated by using ACS data, R is acceleration factor, j is the target coil interpolated by all other coils counted by l , and b and h construct the interpolation kernel. The indices

Yuchou Chang is with the Department of Computer and Information Science at University of Massachusetts Dartmouth, North Dartmouth, MA 02047 USA (phone: 508-999-8475; e-mail: ychang1@umassd.edu).

Ukash Nakarmi is with the Department of Computer Science and Computer Engineering at University of Arkansas, Fayetteville, AR 72701 USA (e-mail: unakarmi@uark.edu).

k_x and k_y represent data positions along frequency encoding and phase encoding directions, respectively.

The interpolation coefficients are calculated at first by using ACS data acquired in k-space. Then, those estimated coefficients are used to interpolate missing k-space data. It can be considered as a linear regression model with complex values of k-space data for solving the linear inverse problem. However, the linear regression model cannot reconstruct missing data exactly [16, 17], since a finite set of acquired data is provided and those acquired data also have noise and outliers produced from data acquisition hardware.

B. Broad Learning System

Broad learning system [13] is a neural network architecture which is not dependent on deep structures. Distinct from many layers in deep learning, broad learning doesn't have enormous connections among hierarchical structure of layers, so its structure is concise and transparent. To enhance accuracy of classification and regression tasks, broad learning system increases the width of its network structure rather than deepening network structure in deep learning models. Additional computational burden in expanding neural nodes broadly is a tiny small portion in compared to that computational cost in increasing depth of the stacked layer-structure. BLS is good at classification and regression tasks with a small amount of training data, fast speed requirements, and real-time incremental learning applications.

BLS was derived from the random vector functional link neural network (RVFLNN) [14], which doesn't need gradient decent to update weights. Instead of using backpropagation to update kernels and weights in CNN, broad learning updates weights of feature-node layer and enhancement-node layer by using the pseudoinverse method. Those node layers in BLS are different from layers in deep neural network, since feature-node layer and enhancement-node layer are not coupled and network structure is concise. Without hierarchically cascaded connections, computation speed of feature-node and enhancement-node layers is much faster than deep neural network speed. Both feature-nodes and enhancement-nodes are inputs of the neural network, which can be expanded to contain new-incoming data or incremental increase of randomly mapped features. BLS is different from Extreme Learning Machine (ELM) [15], since there are connections between input and output layers in BLS but ELM has hidden layers between both of input and output layers.

III. BROAD LEARNING SYSTEM FOR GRAPPA RECONSTRUCTION

The characteristics of broad learning system make it possible to reconstruct missing k-space data through training an interpolation model with a small amount data. A framework of the proposed BLS based GRAPPA reconstruction is presented in Figure 1. ACS data and undersampled k-space data are input into the neural network in autocalibration phase and interpolation phase, respectively. The output layer has ACS data in autocalibration phase and estimations for missing k-space data in interpolation phase.

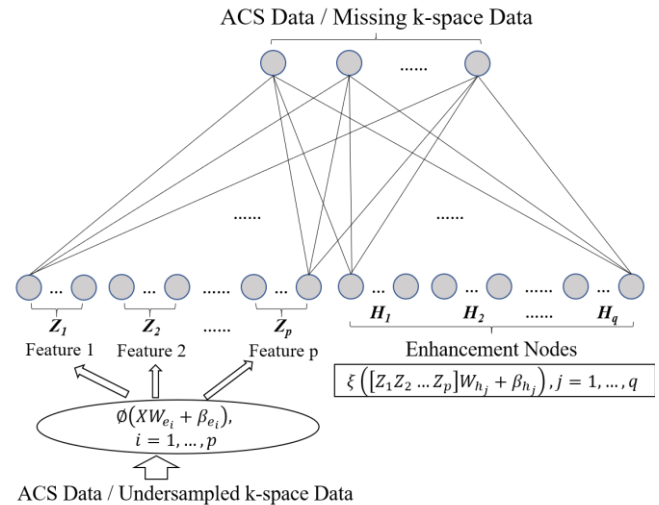


Figure 1. Framework of broad learning system for GRAPPA reconstruction.

A. Feature-Node Layer Generated from k-space Data

Autocalibration signal data is acquired from central k-space for GRAPPA reconstruction. ACS data are assigned to input and output layers of BLS for training the regression model. A linear transformation is applied on ACS data and then fed into feature-node layers as inputs of BLS network. Linear transformation makes raw k-space data in the mapped feature space. Each feature node Z is generated by a linear feature mapping by the random weights W_e with proper dimensions as the following equation:

$$Z_i = \phi(XW_{e_i} + \beta_{e_i}), i = 1, \dots, p \quad (2)$$

, where ϕ is the linear mapping that transforms input k-space data X into mapped features, β is supposed to be randomly generated with the same distribution of W_e . The BLS takes the advantages of sparse autoencoder characteristics to produce the better features.

Since k-space data are complex values rather than real values, those complex values are directly fed into BLS network without changing magnitude and phase information in the proposed method. Unlike deep learning based pMRI reconstruction which used MRI databases acquired from different hardware configurations, only acquired ACS data during the scan are used as training data to be fed into BLS network and then missing k-space data are interpolated using undersampled k-space data. Both training data and testing data are acquired from the same scan, and therefore they have the same distributions and anatomical areas.

B. Nonlinearity Produced by Enhancement Nodes

Since the feature nodes are generated by a linear transform of the original input k-space data, enhancement nodes can provide nonlinear information to characterize nonlinear noise and outliers in k-space data. Since nonlinear relationship between undersampled k-space data and missing data can improve GRAPPA reconstruction quality [16], enhancement-node layer incorporating nonlinearity in regression may also improve interpolation accuracy and enhance reconstruction quality. For this reason, enhancement nodes add nonlinearity into the GRAPPA interpolation process and may improve reconstruction quality.

Feature nodes are nonlinear transformed into enhancement nodes as

$$H_q = \xi \left(Z^p W_{h_q} + \beta_{e_q} \right) \quad (3)$$

, where ξ is a nonlinear activation function [18], and W_{h_q} represents enhancement weight matrix with bias function β_{e_q} . Nonlinearity is incorporated in Equation (3) to increase approximation capability. Different from feature nodes, enhancement nodes don't have sparse representation. Enhancement nodes enhance representation ability to describe input data and make accurate interpolation. All feature nodes and enhancement nodes are connected to output layers, and those connection weights can be computed by using Ridge regression of the pseudoinverse. Through broad expansion in feature nodes and enhancement nodes, incremental learning can be developed by adding new connections and updated their weights.

C. Pseudoinverse for Reconstruction Missing k -space Data

To obtain the mapping between input and output layers, pseudoinverse is used in BLS to compute weights. Let's make A represent the expanded input matrix consisting of all input k -space data mapped vectors combined with enhancement components. If a new enhancement node is added to the network, it is equivalent that a new column is added to the original input matrix A_n , which has the $n \times m$ pattern matrix structure [13]. The n represents total number of feature- and enhancement-nodes, and m is the number of input patterns. The new pattern matrix A_{n+1} by adding a new enhancement node can be represented as

$$A_{n+1} \triangleq [A_n | a]. \quad (4)$$

The pseudoinverse of new pattern matrix is calculated by

$$A_{n+1}^+ = \begin{bmatrix} A_n^+ - db^T \\ b^T \end{bmatrix} \quad (5)$$

, where $d = A_n^+ a$, and

$$b^T = \begin{cases} (c)^+ & \text{if } c \neq 0 \\ (1 + d^T d)^{-1} d^T A_n^+ & \text{if } c = 0 \end{cases} \quad (6)$$

, and $c = a - A_n d$. The new weights are calculated as

$$W_{n+1} = \begin{bmatrix} W_n - db^T Y_n \\ b^T Y_n \end{bmatrix} \quad (7)$$

, where Y_n are output data, and W_{n+1} are updated weights after new enhancement nodes are added based on previous weights W_n .

Weights of connections between output layers and both of feature nodes and enhancement nodes are calculated and updated by pseudoinverse. Missing k -space data are estimated and filled out to produce full k -space data. Inverse Fourier transform is applied on each coil to generate each coil image and then all coil images are combined together for reconstructing the final image, as the traditional GRAPPA does.

IV. EXPERIMENTAL RESULTS

The proposed BLS based GRAPPA reconstruction is evaluated by two in-vivo datasets. The reconstructed images are compared to reference images and the traditional GRAPPA

reconstructed images. The experimental procedures involving human subjects described in this paper were approved by the Institutional Review Board.

A. Datasets

The first dataset contains cardiac images were acquired using a 2D trueFISP sequence (TE/TR 1.87/29.9 ms, bandwidth 930 Hz/pixel, 50 degree flip angle, 6mm slice thickness, 34 cm FOV in readout direction, 256 x 216 acquisition matrix) with a 4-channel cardiac coil. It is undersampled by reduction factor 4 and 64 ACS lines. The reconstruction kernel size is 4 x 15. The second one is a 4-coil brain dataset with the reduction factor 2 and 32 ACS lines. The reconstruction kernel size is 4 x 61. The reconstruction code was implemented in MATLAB (Natick, MA).

B. Reconstruction Quality Evaluation

The first cardiac MRI data are reconstructed by both of the traditional GRAPPA as shown in Figure 2(b) and the proposed broad learning system-based GRAPPA reconstruction as shown in Figure 2(c). Fully sampled k -space was reconstructed as the reference image in Figure 2(a). A patch is extracted and evaluated for reconstruction performance comparison. It can be seen that the proposed BLS based GRAPPA reconstruction outperforms the traditional GRAPPA reconstruction by suppressing noise.

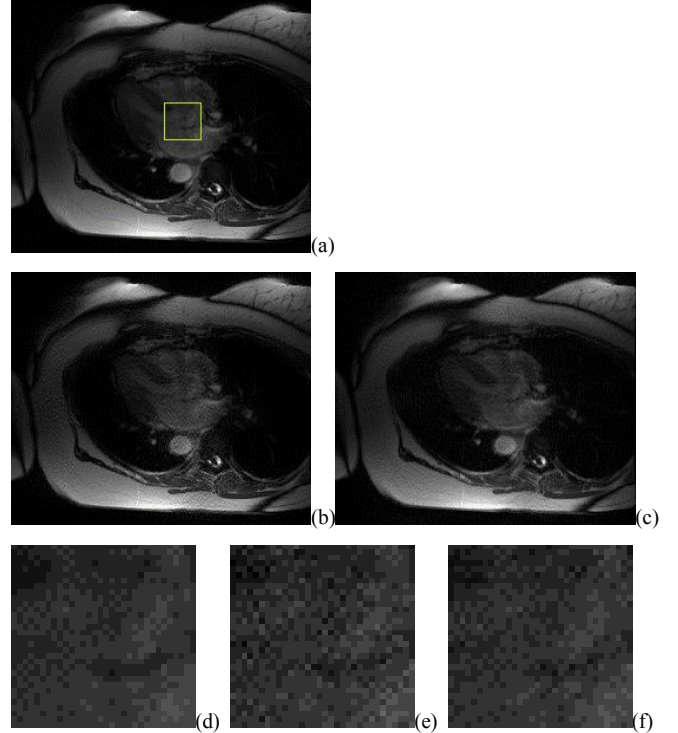


Figure 2. Cardiac MRI reconstruction with the reference image (a), the traditional GRAPPA (b) and the proposed BLS based GRAPPA reconstruction (c). Patches are extracted from reference image (d), GRAPPA reconstruction (e), and BLS based GRAPPA reconstruction (f) for evaluating reconstruction quality.

The second brain dataset was reconstructed by both of the traditional GRAPPA in Figure 3(b) and the proposed BLS based GRAPPA reconstruction in Figure 3(c), respectively. The fully sampled k -space was also reconstructed as the reference image as shown in Figure 3(a). The BLS based

GRAPPA reconstruction also has higher SNR than that of the traditional GRAPPA reconstruction.

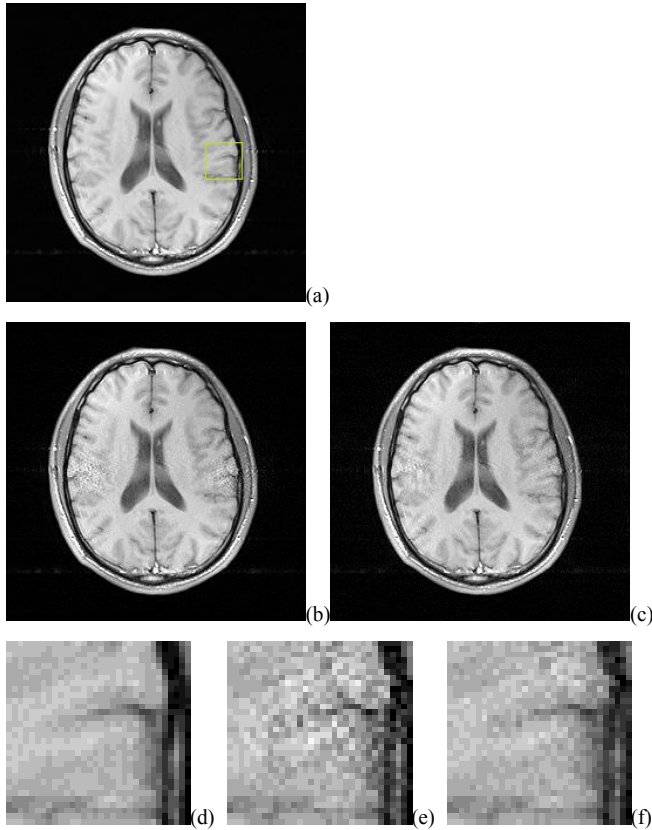


Figure 3. Brain MRI reconstruction with the reference image (a), the traditional GRAPPA (b) and the proposed BLS based GRAPPA reconstruction (c). Patches are extracted from reference image (d), GRAPPA reconstruction (e), and BLS based GRAPPA reconstruction (f) for evaluating reconstruction quality.

The Normalized Mean Square Error (NMSE) are calculated for the traditional GRAPPA reconstruction and BLS based GRAPPA reconstruction, where the latter one is lower than GRAPPA reconstruction NMSE for cardiac and brain images, as shown in the Table I.

TABLE I. NORMALIZED MEAN SQUARE ERROR (NMSE) OF RECONSTRUCTIONS

	Normalized Mean Square Errors	
	Cardiac Reconstruction	Brain Reconstruction
GRAPPA	2.4323e-05	1.0554e-05
BLS	1.3076e-05	5.4897e-06

C. Computational Costs

For the cardiac reconstruction, the traditional GRAPPA and BLS need 4.5 seconds and 229.3 seconds, respectively, respectively. Furthermore, the computational times are 28.6 seconds and 191.9 seconds for GRAPPA reconstruction and BLS based GRAPPA reconstruction of the brain dataset. Although BLS based reconstruction is longer than the traditional GRAPPA reconstruction, it is still faster than

training time of MRI reconstruction using deep learning approaches which require a large amount of MRI data.

V. CONCLUSION

In conclusion, the broad learning system is studied and applied on GRAPPA reconstruction. Broad learning doesn't need deep architectures of deep learning models, and therefore reduce computational costs of training a model on a large amount of MRI data, as well as avoid a large hyperparameter tuning workload. In the proposed method, training data and testing data acquired from the same scan of with the same configuration profile to avoid transfer learning between training data and testing data. The proposed method is able to enhance reconstruction quality by reducing noise in compared to the traditional GRAPPA reconstruction. Future work will focus on dynamic parallel MRI reconstruction with incremental learning characteristics of broad learning system.

REFERENCES

- [1] Z.P. Liang and P.C. Lauterbur, "Principles of magnetic resonance imaging: a signal processing perspective," 1st ed. Wiley-IEEE Press, 1999.
- [2] J. Hamilton, D. Franson, and N. Seiberlich, "Recent advances in parallel imaging for MRI," *Prog. Nucl. Magn. Reson. Spectrosc.*, vol. 101, pp.71-95, 2017.
- [3] K.P. Pruessmann, M. Weiger, M.B. Scheidegger, P. Boesiger, "SENSE: sensitivity encoding for fast MRI," *Magn. Reson. Med.*, vol. 42, no. 5, pp. 952-962, 1999.
- [4] M.A. Griswold, P.M. Jakob, R.M. Heidemann, N. Mathias, V. Jellus, J. Wang, B. Kiefer, and A. Haase, "Generalized autocalibrating partially parallel acquisitions (GRAPPA)," *Magn. Reson. Med.*, vol. 47, pp. 1202-1210, 2002.
- [5] M. Lustig and J.M. Pauly, "SPIRiT: Iterative self-consistent parallelimaging reconstruction from arbitrary K-space," *Magn. Reson. Med.*, vol. 64, no. 2, pp. 457-471, 2010.
- [6] M. Akçakaya, S. Moeller, S. Weingärtner, and K. Ugürbil, "SENSE: sensitivity encoding for fast MRI," *Magn. Reson. Med.*, vol. 81, no. 1, pp. 439-453, 2019.
- [7] J.Y. Cheng, M. Mardani, M. T. Alley, J.M. Pauly, and S.S. Vasanawala, "Deep-SPIRiT: generalized parallel imaging using deep convolutional neural networks," *In Proc. 26th Annual Meeting of the ISMRM*, Paris, France, 2018.
- [8] Y. Han, L. Sunwoo, and J. C. Ye, "k-space deep learning for accelerated MRI," *IEEE Trans. Medical Imaging*, vol. 39, no. 2, pp. 377-386, 2020.
- [9] D. Liang, J. Cheng, Z. Ke, and L. Ying, "Deep magnetic resonance image reconstruction: inverse problems meet neural networks," *IEEE Signal Processing Magazine*, vol. 37, no. 1, pp. 141-151, 2020.
- [10] F. Knoll, et al., "fastMRI: a publicly available raw k-space and DICOM dataset of knee images for accelerated MR image reconstruction using machine learning," *Radiol Artif Intell.*, PMID: PMC6996599, 2020.
- [11] S.J. Pan and Q. Yang, "A survey on transfer learning," *IEEE Trans. Knowledge and Data Engineering*, vol. 22, no. 10, pp. 1345-1359, 2010.
- [12] F. Knoll, K. Hammernik, E. Kobler, T. Pock, M.P. Recht, and D.K. Sodickson, "Assessment of the generalization of learned image reconstruction and the potential for transfer learning," *Magn. Reson. Med.*, vol. 81, pp. 116-128, Jan 2019.
- [13] C.L.P. Chen and Z. Liu, "Broad learning system: an effective and efficient incremental learning system without the need for deep architecture," *IEEE Trans. Neural Networks and Learning Systems*, vol. 29, no. 1, pp. 10-24, 2017.
- [14] Y.H. Pao and Y. Takefuji, "Functional-link net computing: theory, system architecture, and functionalities," *Computer*, vol. 25, no. 5, pp. 76-79, 1992.
- [15] G. B. Huang, Q. Y. Zhu, and C. K. Siew, "Extreme learning machine: theory and applications," *Neurocomputing*, vol. 70, no. 1-3, pp.489-501, 2006.
- [16] Y. Chang, D. Liang, and L Ying, "Nonlinear GRAPPA: A kernel approach to parallel MRI reconstruction," *Magn. Reson. Med.*, vol. 68, no. 3, pp. 730-740, 2012.
- [17] J. Lyu, Y. Chang, and L Ying, "Fast GRAPPA reconstruction with random projection," *Magn. Reson. Med.*, vol. 74, no. 1, pp. 71-80, 2015.
- [18] C.L.P. Chen and J.Z. Wan, "A rapid learning and dynamic stepwise updating algorithm for flat neural networks and the application to time-series prediction," *IEEE Trans. Systems, Man, and Cybernetics, Part B (Cybernetics)*, vol. 29, no. 1, pp. 62-72, 1999.